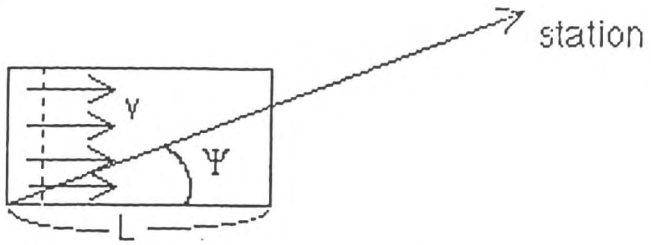

Fig. 1.36: Directivity of a finite fault.

In this case, we can write

$$\phi_f = \frac{\omega L}{2}\left[\frac{1}{v} - \frac{\cos\Psi}{c}\right] + \omega\tau_D$$

where L is the fault length, v is the rupture velocity, Ψ is the angle between the ruputre direction and the azimuth to the observation point, and τ_D is the time delay due to the inital break of the fault. This phase term $\phi_f(\omega)$ is negligible for earthquakes of small fault area.

Although we need the above additional information on source process for the single station method, there are no constraints on station locations unlike other methods, which makes this approach very popular in present.

1.4 Estimation of Velocity Structure from Phase (Group) Velocity Observation

Once we get a dispersion curve $C(\omega)$ or $U(\omega)$ using the techniques described in the previous chapter, we like to obtain the velocity structure of the earth as a function of depth $v(z)$ with the relation between them:

$$\underset{\text{model}}{v(z)} \leftrightarrow \underset{\text{observation}}{C(\omega), U(\omega)}$$

As touched upon before regarding the origin of the dispersive character of surface waves, the above relationship is based on the difference of energy profiles of frequencies in accordance with depth. In short period surface waves, most of the energy is trapped near the free surface, which reflects the velocity structure at shallow depths. By contrast, the energy of long period surface waves penetrates into deeper parts and such waves contain information on the deep velocity structure (Fig. 1.37).

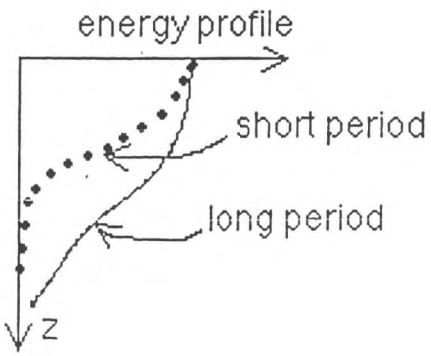

Fig. 1.37: Energy profile of surface waves.

Because of the characters described in the beginning of this note, Love and Rayleigh waves should reflect the following parameters of the earth:

$$\begin{cases} \text{Love wave (SH type)} & \ldots \beta(z) \text{ and } \rho(z) \\ \text{Rayleigh wave (P-SV type)} & \ldots \beta(z),\ \alpha(z) \text{ and } \rho(z) \end{cases}$$

although the density $\rho(z)$ is rather insensitive to the dispersive character.

(a) Forward modelling

First, we shall discuss forward modelling: a model $v(z)$ is given and we then compute dispersion curves $C(\omega)$ (and $U(\omega)$). Here we explain only the Love wave case because it is much simpler than the Rayleigh wave case.

Let us consider a plane Love wave propagating in the x-direction with frequency ω. The polarization plane is therefore along the y axis (Fig. 1.38), and we can write displacement components as follows:

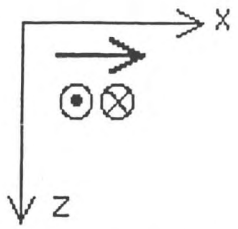

Fig. 1.38: Love wave propagation in the *x* direction.

$$u = w = 0,$$
$$v = \ell_1(\omega, k : z)e^{i(kx-\omega t)}$$

where ℓ_1 represents the vertical energy profile, and the resulting stress tensor is expressed by

$$\tau_{xx} = \tau_{yy} = \tau_{zz} = \tau_{zx} = 0,$$
$$\tau_{yz} = \mu\left(\frac{\partial v}{\partial z} + \frac{\partial w}{\partial y}\right) = \mu\frac{d\ell_1}{dz}e^{i(kx-\omega t)},$$
$$\tau_{xy} = \mu\left(\frac{\partial v}{\partial x} + \frac{\partial u}{\partial y}\right) = ik\mu\ell_1 e^{i(kx-\omega t)}.$$

Inserting the above relations to the elastodynamic equation:

$$\rho\ddot{u}_i = \frac{\partial \tau_{ji}}{\partial x_j} \quad \text{(Note that here only } i = 2 \text{ is non-zero.)}$$

or in this case

$$\rho\ddot{v} = \frac{\partial \tau_{yx}}{\partial x} + \frac{\partial \tau_{yy}}{\partial y} + \frac{\partial \tau_{yz}}{\partial z},$$

and we obtain

$$-\omega^2\rho(z)\ell_1 = \frac{d}{dz}\left[\mu(z)\frac{d\ell_1}{dz}\right] - k^2\mu(z)\ell_1.$$

This is a second-order linear ordinary differential equation, which can be easily solved numerically, while the original elastodynamic equation is a partial differential equation which is too difficult to be solved directly.

It is better to transform this equation into two first-order linear differential equations for ease of numerical treatment. For this purpose, let us introduce ℓ_2 as

$$\tau_{yz} = \mu \frac{d\ell_1}{dz} e^{i(kx-\omega t)} \equiv \ell_2 e^{i(kx-\omega t)},$$

we then get

$$\begin{cases} \dfrac{d\ell_1}{dz} = \dfrac{\ell_2}{\mu(z)} \\ \dfrac{d\ell_2}{dz} = (k^2\mu(z) - \omega^2\rho(z))\ell_1 \end{cases}$$

or in matrix form

$$\frac{d}{dz}\begin{pmatrix} \ell_1 \\ \ell_2 \end{pmatrix} = \begin{pmatrix} 0 & \mu(z)^{-1} \\ k^2\mu(z) - \omega^2\rho(z) & 0 \end{pmatrix}\begin{pmatrix} \ell_1 \\ \ell_2 \end{pmatrix}.$$

Boundary conditions for the present functions ℓ_1 and ℓ_2 are as follows:

$$\begin{cases} \ell_1 \to 0 & \text{as } z \to \infty \quad \text{(energy decaying in depth)} \\ \ell_2 = 0 & \text{at } z = z_0 \quad \text{(traction-free at the surface)} \\ \ell_1, \ell_2 & : \quad \text{continuous.} \end{cases}$$

With these boundary conditions, we shall solve the above linear differential equations numerically. We start the integration of these equations with one initial value of $k = \omega / C(\omega)$ to obtain the values of ℓ_1 and ℓ_2 at the surface. ℓ_2=0 is generally not given there, as it does not satisfy the boundary condition at the surface, so we select a different value of k, then start the integration again. We repeat this process by correcting the value of k until we get a value of ℓ_2 at the surface sufficiently close to zero, which gives the actual phase velocity $C(\omega)$. (See Takeuchi and Saito (1972) for various numerical techniques.) For Rayleigh waves, we need more complicated formulations but essentially we obtain four first-order differential equations in contrast with two for Love waves (see chapter 7.3 of Aki and Richards (1980)).

Table 1.1 and Fig. 1.39-41 give the Gutenberg Earth model with its dispersion curves and vetical energy profiles of eigenfunctions. You can easily understand the change of vertical energy profile as frequency or period is changed.

Computed values of phase velocity values computed with an assumed velocity model would be different from observed ones. We would like to improve the model to decrease such discrepancies in the dispersion curve. Since short period waves are dominated only by shallow parts, we should increase the velocity values at shallow parts if we want to get higher phase velocities in a short period range. On the other hand, we should increase velocities at great depth to get higher phase velocities for long period surface waves (Fig. 1.42). We often repeat this tryal-and-error procedure until we get satisfactory agreement between the predicted values of a model and the observed ones. This is called forward modelling.

Layer number	*Depth to bottom* (km)	*density* (g/cm^3)	v_p (km/sec)	v_s (km/sec)
1	19	2.74	6.14	3.55
2	38	3.00	6.58	3.80
3	50	3.32	8.20	4.65
4	60	3.34	8.17	4.62
5	70	3.35	8.14	4.57
6	80	3.36	8.10	4.51
7	90	3.37	8.07	4.46
8	100	3.38	8.02	4.41
9	125	3.39	7.93	4.37
10	150	3.41	7.85	4.35
11	175	3.43	7.89	4.36
12	200	3.46	7.98	4.38
13	225	3.48	8.10	4.42
14	250	3.50	8.21	4.46
15	300	3.53	8.38	4.54
16	350	3.58	8.62	4.68
17	400	3.62	8.87	4.85
18	450	3.69	9.15	5.04
19	500	3.82	9.45	5.21
20	600	4.01	9.88	5.45
21	700	4.21	10.30	5.76
22	800	4.40	10.71	6.03
23	900	4.56	11.10	6.23
24	1000	4.63	11.35	6.32

Table 1.1: Gutenberg model of continental structure [Aki and Richards, 2002] (published by University Science Books).

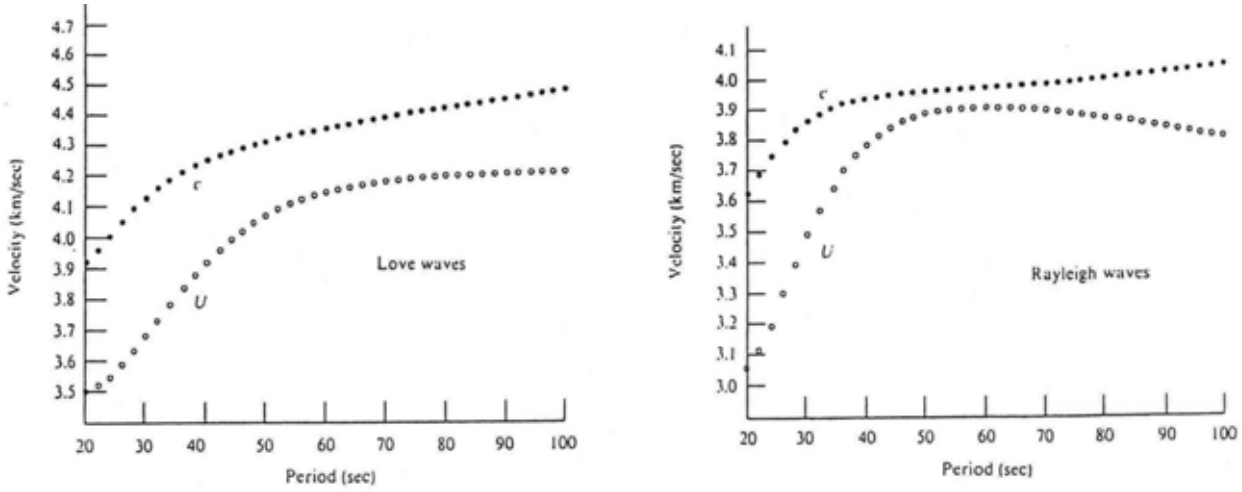

Fig.1.39: Phase and group velocities of the fundamental-mode Love and Rayleigh waves for the Gutenberg Earth model [Aki and Richards, 2002] (published by University Science Books).

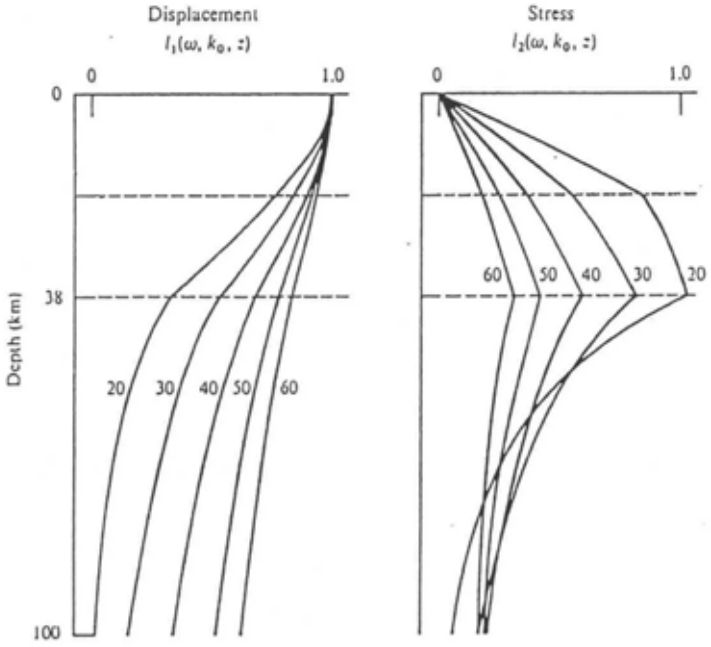

Fig.1.40: The eigenfunctions for the fundamental-mode Love waves [Aki and Richards, 2002] (published by University Science Books).

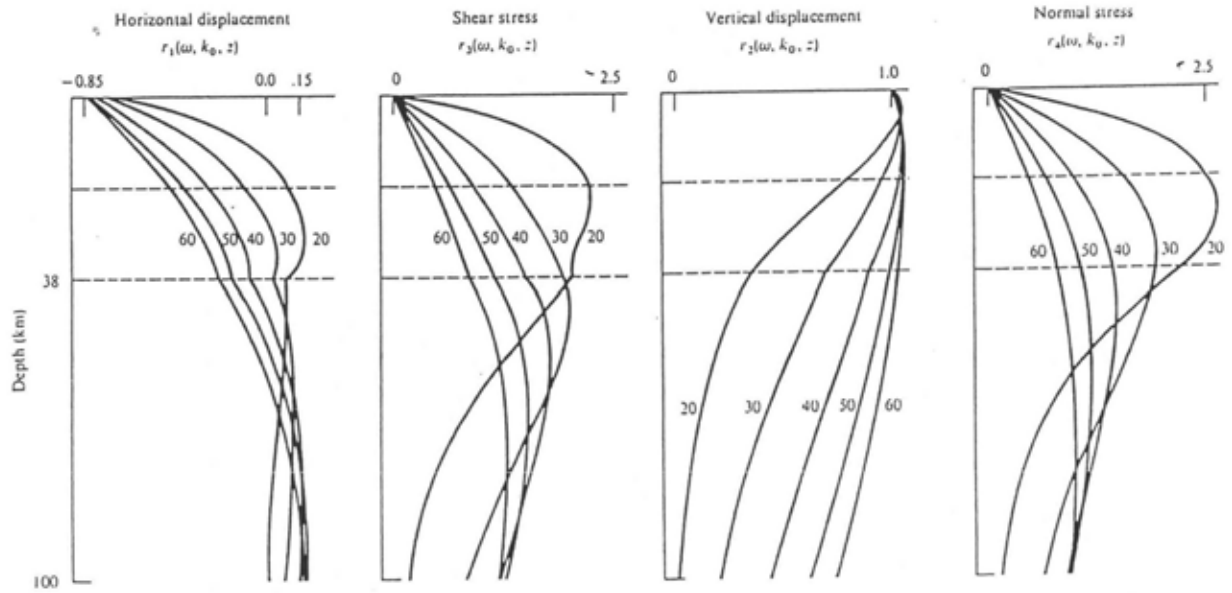

Fig.1.41: The eigenfunctions for the fundamental-mode Rayleigh waves [Aki and Richards, 2002] (published by University Science Books).

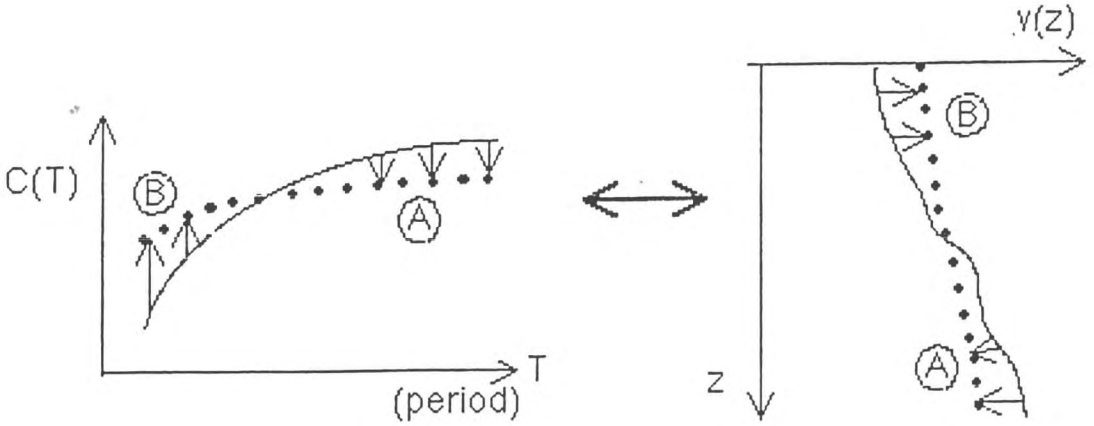

Fig. 1.42: Relationship between the phase velocity dispersion curve and velocity structure to depth.

(b) Inverse Problem

Instead of the above tryal-and-error procedure, we want to carry out a more systematic model change in order to efficiently obtain satisfactory results. That is, we would like to find the relationship betwen the difference of an observed velocity value from a model-predicted one $\delta C\,(\omega)$, and the correction of velocity in structure for the next step $\delta v\,(z)$:

$$\delta C\,(\omega) = C_{obs}\,(\omega) - C_{pred}\,(\omega) \leftrightarrow \delta v\,(z)$$

we then use a new velocity model with $v_0(z) + \delta v\,(z)$ at the following step where $v_0\,(z)$ is the velocity model at the previous step. Correcting the model with the above procedure is generally called an inverse problem.

In the case of surface waves, it is very important that as long as velocity perturbation $\delta v\,(z)$ is sufficiently small, we can set up a linear relationship between $\delta C\,(\omega)$ and $\delta v\,(z)$. In the case of Love waves, such a relationship can be expressed in the following form:

$$\left(\frac{\delta C}{C}\right)_{\omega} = -\frac{\delta k}{k} = \frac{\int_0^{\infty}\left[k^2\ell_1^2 + \left(\frac{d\ell_1}{dz}\right)^2\right]\delta\mu(z)dz - \int_0^{\infty}\omega^2\ell_1^2\delta\rho(z)dz}{2k^2\int_0^{\infty}\mu\ell_1^2 dz}$$

which represents that the correction of the model $\delta\mu\,(z)$ or $\delta\rho\,(z)$ is propotional to the discrepancy in phase velocity δC between a model-predicted one and an observation. For the derivation of this relationship and other formulations such as Rayleigh waves, please refer to Takeuchi and Saito (1972).

1.5 Regional Variation of Surface Wave Propagation

In the final chapter, we shall look through velocity structures in various regions all over the world, estimated from surface wave analyses (for examples, refer to Knopoff, 1972). We shall pay attention to the relationship between velocity structures and dispersion curves in each region. One of the most significant lateral heterogeneities on the global scale is the difference between oceans and continents, although there are strong variations within a particular ocean or a particular continent, as shown later. It is rather cumbersome to review regional variations at every area in the world, so let us just take several typical applications of regional variations in velocity structure to suface waves.

(a) Low velocity zone

First of all, we look at two classical earth models: the models of Jeffreys and Gutenberg established already in 1920's. These models were obtained by travel time studies mainly of P and S waves. The two models agree very well except for a few parts. One major discrepancy is that the velocity increases monotonously with depth in the upper mantle for the Jeffreys model while there is a low velocity zone (LVZ) at a depth of around 100 ~ 200 km in the Gutenberg model. It is very difficult to judge which model is superior from travel time observations (see "Ray Theory" in this lecture series). Fig.1.43 shows these models and their dispersion curves of Rayleigh waves, which were first obtained around 1960 when computers were available to geophysicists for the first time. The effect of LVZ on the dispersion curves is clearly seen, particularly for group velocities with periods of around 100 to 250 sec. Observations agree with the Gutenberg model rather than the Jeffery model, which implies that the LVZ indeed exists.

(b) The size of the low velocity zone

The next question is how significant the low velocity zone is or how much velocity is reduced within the LVZ. Dorman et al. (1960), who showed the first evidence of the existence of LVZ as dicussed in the previous example, computed dispersion curves for several ocean models with various degrees of LVZ, as shown in Fig.1.44. Model 8099 has a larger LVZ than model 8096 and the former agrees well with the observations, particularly in group velocities with periods of over 100 sec. We therefore consider that most oceanic areas have an LVZ as significant as that of model 8099.

(c) Continent vs Ocean

As explained earlier, one of the most significant variations in the regionality of velocity structures is the diffrence between continents and oceans. From oceanic refraction experiments by Ewing and others in 1940's, it is apparent that the oceanic crust is much thinner (less than 10 km) than the continental crust (about 35 km). We expect that some significant difference can be seen in dispersion curves of surface waves. Fig.1.45 compares two models obtained, one called 8099 for oceans, which was explained above, and the other called CANSD estimated for the Canadian Shield, one of the oldest and stablest continental areas of the world, studied by Brune and Dorman (1962). Phase velocity dispersion curves of Rayleigh waves for both models are compared and it is apparent that there is a crossover in dispersion curves at a period of around 30 sec: in longer period range, CANSD gives higher values of phase velocity, and for shorter periods vice versa. This is due to the following major characters of both models:

- CANSD: thick crust (~ 40 km) and no significant LVZ

- 8099: high velocity at the depth shallower than 60 km and a significant LVZ (60 ~ 200 km)

(d) Eurasian continent

Although oceanic and continental areas have a first-order difference in velocity structure, there are also tremendous variations within each area. Here we show such an example taken from Patton (1978) for the Eurasian continent (Fig. 1.46). He divided the studied area into six regions and obtained shear velocity structures from Rayleigh wave phase velocities. As for the case of CANSD, the old Indian Shield has its high phase velocity values over the priod range taken into considerations and it can be characterized with its thick crust and weak LVZ. On the other hand, the areas named "Tectonic" such as the mountains in the Middle East and in northwest China give much lower values in phase velocity, which implies lower velocity in the uppermost mantle as around a depth of 60 km as well as a well-developed LVZ. However, the most anomalous

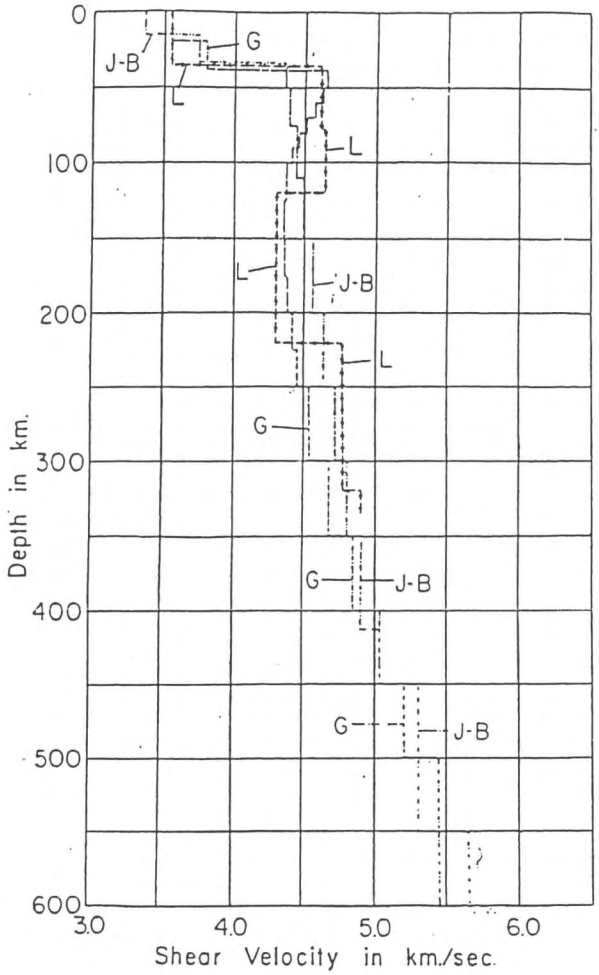

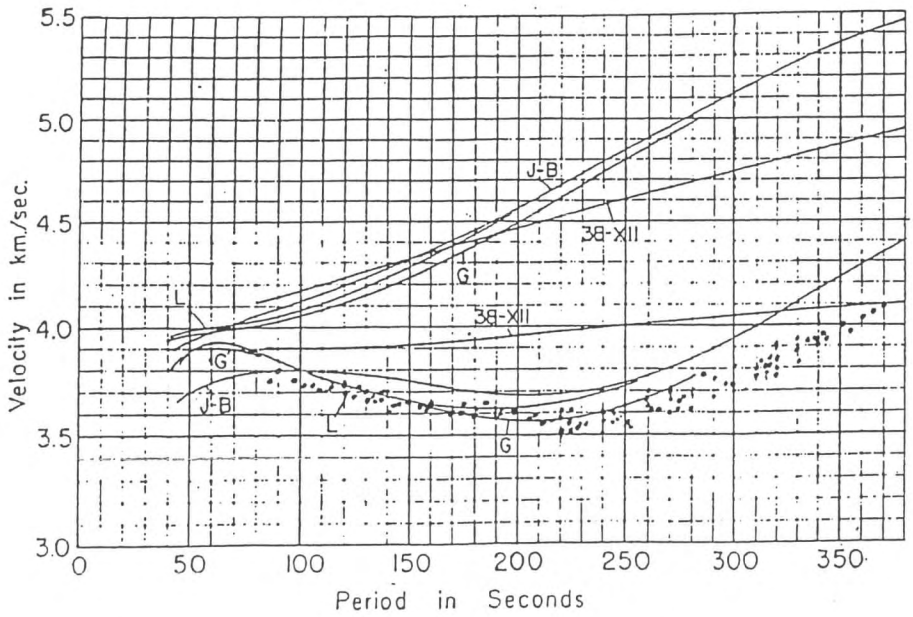

Fig. 1.43: Shear wave velocity structures and corresponding Rayleigh wave dispersion curves (upper lines: phase velocity, lower lines: group velocity) for the Jeffreys-Bullen (J-B) and the Gutenberg (G) models compared with observed data (dots) [Dorman et al., 1960].

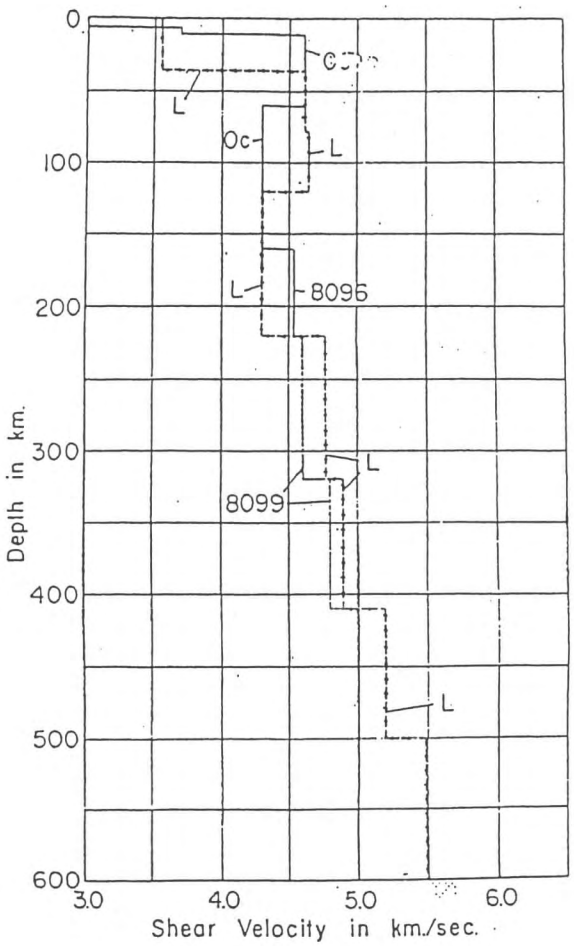

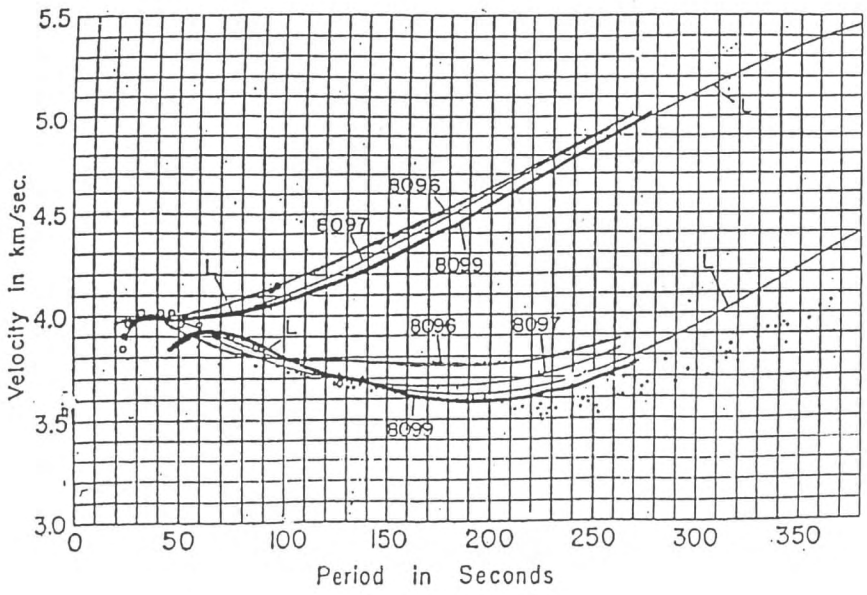

Fig. 1.44: Shear wave velocity structures and corresponding Rayleigh wave dispersion curves (upper lines: phase velocity, lower lines: group velocity) for oceanic models with various degrees of low velocity zone [Dorman et al., 1960].

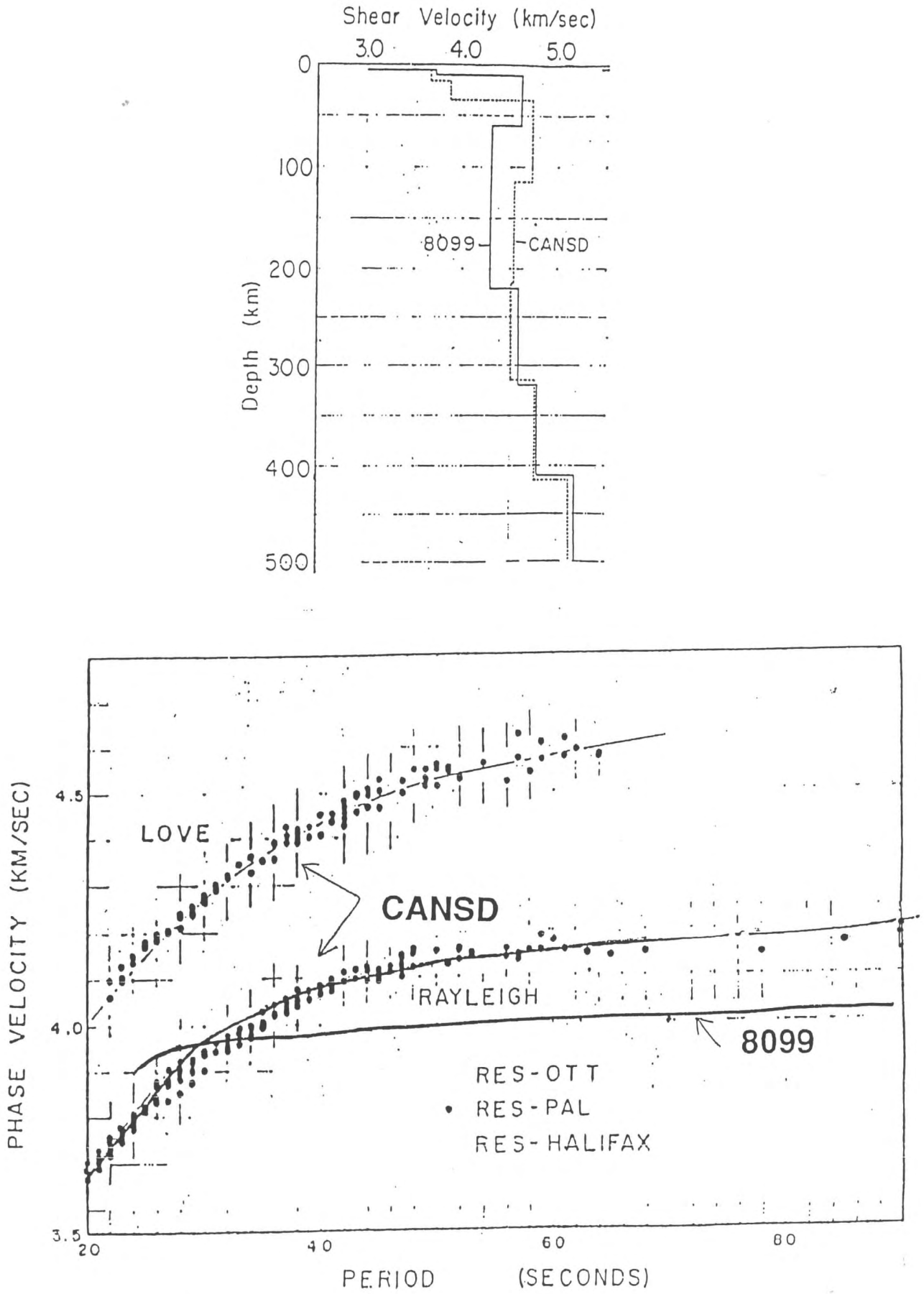

Fig. 1.45: Shear wave velocity structures and corresponding phase velocity dispersion curves for an old-shield model (CANSD) and an oceanic model (8099) [after Brune and Dorman, 1963].

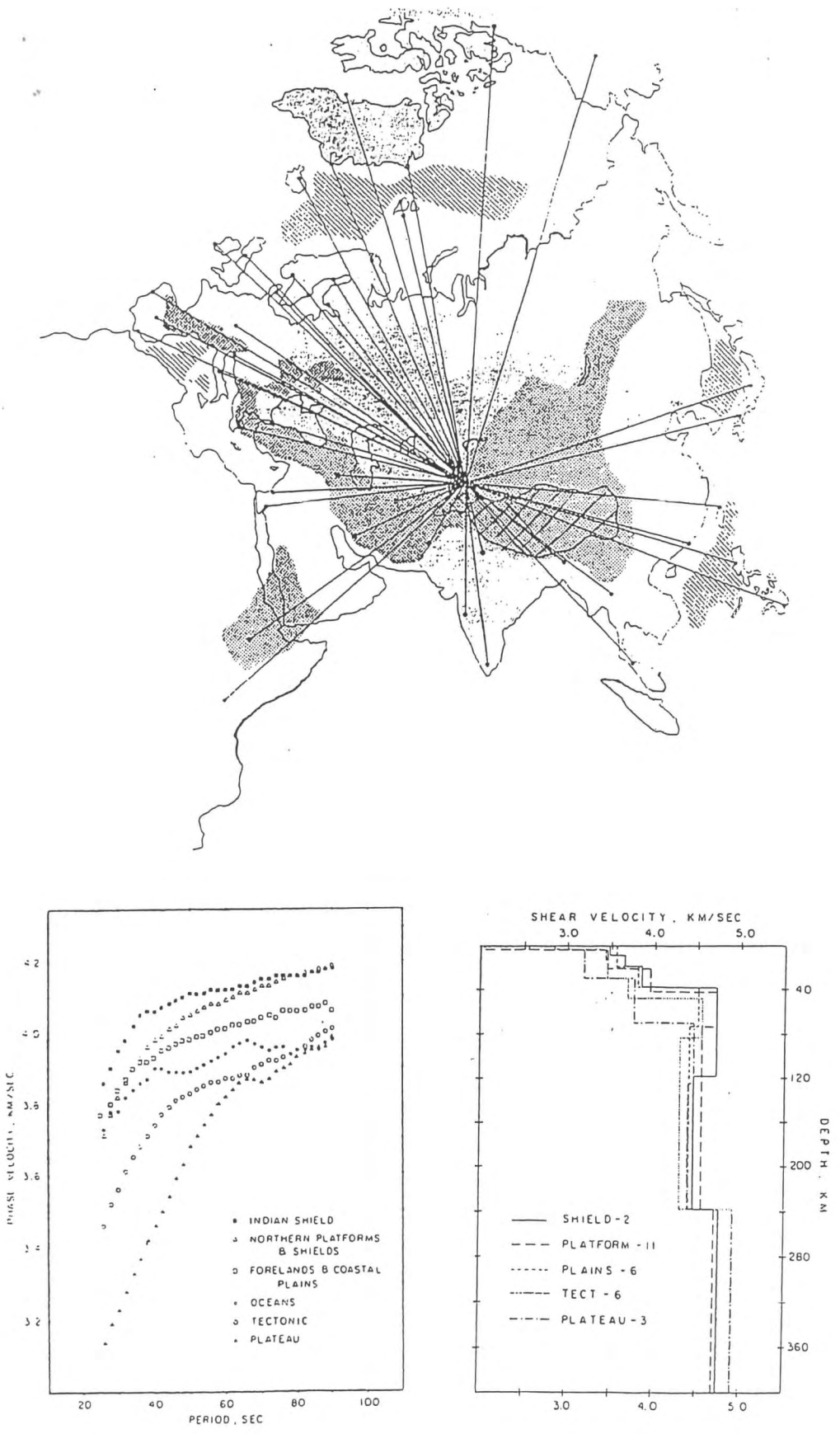

Fig. 1.46: Propagation paths, Rayleigh wave phase velocities, and shear velocity structures of various regionalized areas in and around the Eurasian continent [Patton, 1980]. (Copyright by the American Geophysical Union)

area in this study is the Tibetan Plateau. Phase velocity for this area is very low, particularly in periods shorter than 60 sec, implying that there is a very low velocity surface layer down to quite a large depth extent. Using other observations, a model with the crust of double thickness (over 60 km) is proposed. The Tibetan Plateau is anomalous not only in its low velocity. Fig. 1.47 shows seismograms recorded at three stations for a nuclear explosion located in the north of the Plateau. It is apparent that long period portions of surface waves are strongly attenuated when they pass through the Plateau, from which we guess that the deeper part of the Tibetan Plateau, probably below the bottom of the double-thickness crust, is highly attenuative. This area is one of the most tectonically interesting areas in the world.

(e) **Ocean floor evolution**

Finally, let us look at variations within oceans. Plate tectonics tells us that oceanic floors are created along ocean ridges and move away, spreading laterally to both sides. The ocean floors are cooled down as the distance from ocean ridges increases. Fig. 1.48 and 1.49 are taken from Forsyth (1975, 1977) who studied the oceanic area around the East Pacific Rise because the spreading rate of the ocean floor in this area is one of the fastest in the world and we can easily discern areas of various ages on the ocean floor. Dispersion curves of Rayleigh waves for four ranges of ocean floor age are shown. It is apparent that both phase and group velocities increase as the ocean floor becomes older or cooler. Using such variation in dispersion curves, we can estimate the evolution of ocean floor structure in terms of age, as schematically shown in the last figure. Although the velocity inside the lithosphere increases constantly with age, the thickness of the ocean floor seems to increase abruptly at ages younger than 10 m.y., while it does not change significantly thereafter. This kind of research is very important to study the evolution of lithosphere, which plays a key role in plate tectonics.

Appendix: Formal Definition of Group Velocity

In the main text, we derived the group velocity with waves with only two adjacent frequencies. In this appendix, we shall discuss group velocity in a more general form.

With a single frequency ω, a plane surface wave propagating in the x direction is expressed by a harmonic wave with a phase velocity of $C(\omega)$,

$$(\text{waveform}) \simeq F(\omega, x)e^{-i\omega(t-x/C(\omega))}.$$

The form of surface waves in general is then expressed by the summation of the above element over various frequencies:

$$f(x,t)=\frac{1}{2\pi}\int_{-\infty}^{\infty} F(\omega,x)e^{-i\omega(t-x/C(\omega))}d\omega$$

which is equivalent to an inverse Fourier transform. Although both the amplitude $F(\omega, x)$ and phase $\phi(\omega)$ $(= -\omega(t - x/C(\omega)))$ are continuous in frequency, we approximate them with many piece-wise segments of central frequencies ω_i with a small frequency interval $\Delta\omega$ as shown in Fig. 1.50:

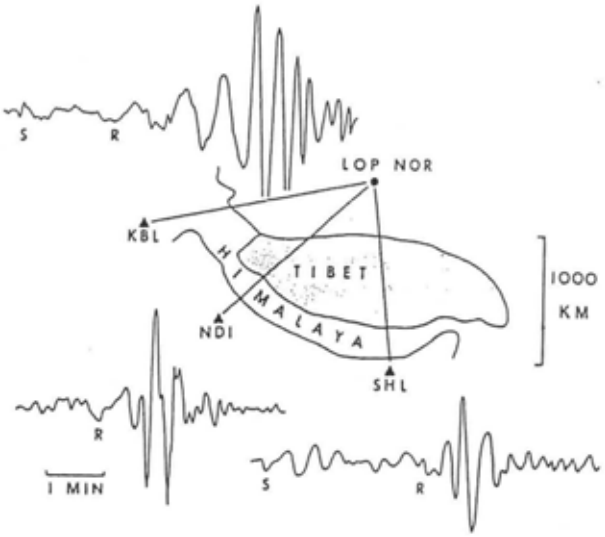

Fig. 1.47: Rayleigh waves recorded from a nuclear explosion at Lop Nor, Xinjiang, propagating through the Tibetan plateau [Toksöz and Bird, 1977]. (Copyright by the American Geophysical Union)

This figure is masked
due to copyright problem.

Fig.1.48: Propagation paths of Rayleigh waves in the East Pacific [Forsyth, 1975].

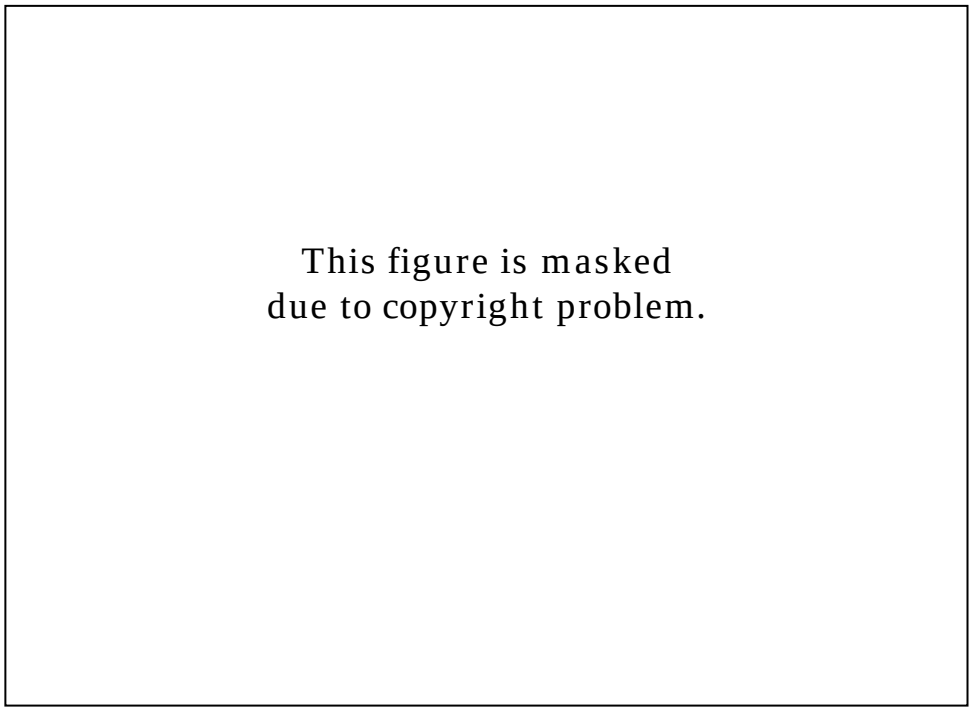

Fig.1.49: Rayleigh wave phase and group velocities as function of the sea floor age given in millions of years, and the obtained evolution model of lithosphere and asthenosphere in young sea floor [Forsyth, 1977].

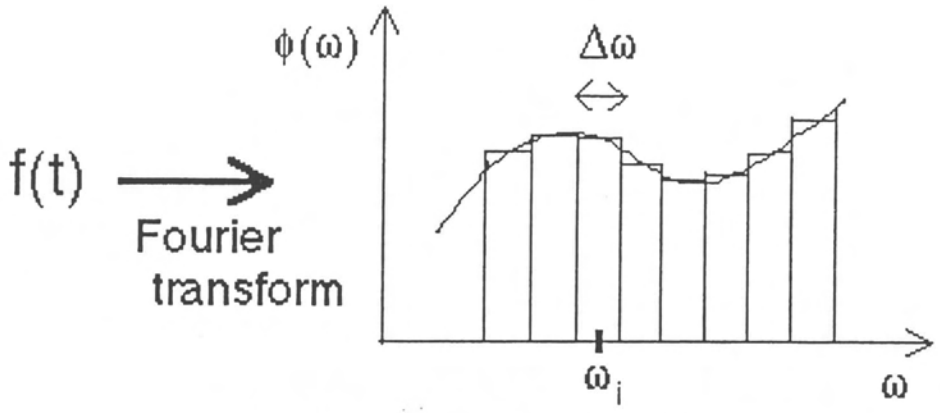

Fig. 1.50: Phase term of seismogram.

We then make the following approximations:

$$\int d\omega \rightarrow \sum_i \int_{\omega_i - \frac{\Delta\omega}{2}}^{\omega_i + \frac{\Delta\omega}{2}} d\omega,$$

$$\frac{\omega}{C(\omega)} \simeq \frac{\omega_i}{C(\omega_i)} + \frac{d}{d\omega}\left(\frac{\omega}{C(\omega)}\right)\Bigg|_{\omega=\omega_i} (\omega - \omega_i) + \cdots$$

then the surface wave is expressed in a time domain by

$$f(x,t) = \frac{1}{\pi}\sum_i F(\omega_i, x) \int_{\omega_i - \Delta\omega/2}^{\omega_i + \Delta\omega/2} \cos\left\{\omega t - \frac{\omega_i x}{C(\omega_i)} - \frac{d}{d\omega}\left(\frac{\omega}{C(\omega)}\right)\Bigg|_{\omega_i} (\omega - \omega_i)x\right\} d\omega.$$

The integration in the above formulation may be written as

$$\int \cos\{\ \}d\omega \equiv \int \cos(\omega T + \psi) d\omega$$

where

$$T \equiv t - \frac{d}{d\omega}\left(\frac{\omega}{C(\omega)}\right)\Bigg|_{\omega_i} x,$$

$$\psi \equiv -\frac{\omega_i x}{C(\omega_i)} + \omega_i \frac{d}{d\omega}\left(\frac{\omega}{C(\omega)}\right)\Bigg|_{\omega_i} x$$

which can be evaluated as follows:

$$\begin{aligned}
\int \cos\{\ \}d\omega &= \frac{\sin(\omega T + \psi)}{T}\Bigg|_{\omega_i - \Delta\omega/2}^{\omega_i + \Delta\omega/2} \\
&= \frac{\sin(\omega_i T + \Delta\omega\, T/2 + \psi) - \sin(\omega_i T - \Delta\omega\, T/2 + \psi)}{T} \\
&= \frac{\sin(\Delta\omega\, T/2)}{T/2}\cos(\omega_i T + \psi) \\
&= \frac{\sin(\Delta\omega\, T/2)}{T/2}\cos\left[\omega_i\left(t - \frac{x}{C(\omega_i)}\right)\right].
\end{aligned}$$

The general surface wave is therefore written as (Fig. 1.51)

$$f(x,t) \simeq \frac{1}{\pi} \sum_i F(\omega_i, x) \Delta\omega \frac{\sin X}{X} \cos\left(\omega_i t - \frac{\omega_i x}{C(\omega_i)} \right)$$

where

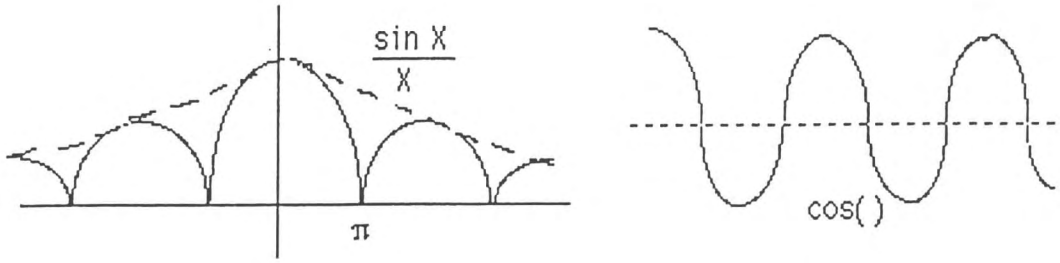

Fig. 1.51: Forms of sin X/X and cos ().

$$X \equiv \frac{\Delta\omega}{2} \left[t - \frac{d}{d\omega} \left(\frac{\omega}{C(\omega)} \right) \Big|_{\omega_i} x \right]$$

$$= \frac{\Delta\omega}{2} \left[t - \frac{x}{U(\omega_i)} \right].$$

with the group velocity at ω_i defined by

$$U(\omega_i) \equiv 1 / \frac{d(\omega / C)}{d\omega} \Big|_{\omega_i} = 1 / \frac{dk}{d\omega} \Big|_{\omega_i} = \frac{d\omega}{dk} \Big|_{\omega_i}.$$

In the i-th component of the above expression, it is easily understood that the peaks and troughs of the waveform propagate with the velocity of $C(\omega_i)$ while the entire wavepacket moves with $U(\omega_i)$ as shown in Fig.1. 52.

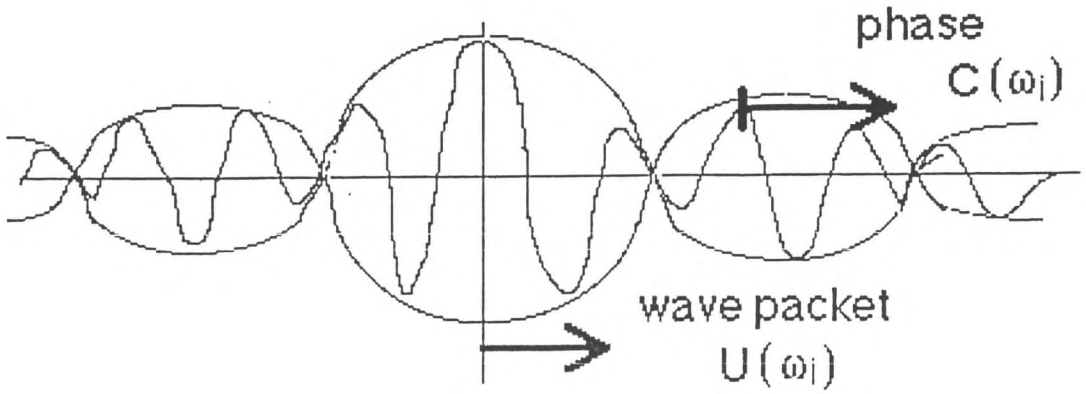

Fig. 1.52: Phase and group velocities with narrow frequency band $\Delta\omega$.

References

PART I

Aki, K., and P. G. Richards, *Quantitative Seismology: Second Edition*, University Science Books, p279-282, 2002.

Aki, K., and P. G. Richards, *Quantitative Seismology: Theory and Methods*, W.H. Freeman,San Francisco, Calif., p259-319, p565-566, p580-584, p586-587, p630-639, 1980.

Bolt, B.A., *Nuclear Explosions and Earthquakes: The Parted Veil*, W.H. Freeman, San Francisco, Calif., 1976.

Brune, J. and J. Dorman, Seismic waves and earth structure in the Canadian Shield, *Bull.Seismol. Soc. Amer.*, *53*, 167-210, 1963.

Dorman, J., M. Ewing, and J. Oliver, Study of shear-velocity distribution in the uppermantle by mantle Rayleigh waves, *Bull. Seismol. Soc. Amer.*, *50*, 87-115, 1960.

Dziewonski, A., and A. Hales, Numerical analysis of dispersed seismic waves, in *Seismology: Surface waves and Earth oscillations (Methods in Computational Physics, vol. 11)*,ed. by B.A. Bolt, Academic Press, New York, 39-85, 1972.

Dziewonski, A., S. Bloch and M. Landisman, A technique for the analysis of transient seismic signals, *Bull. Seismol. Soc. Amer.*, *59*, 427-444, 1969.

Forsyth, D.W., The early structural evolution and anisotropy of the oceanic upper mantle, *Geophys. J. Roy. Astron. Soc.*, *43*, 103-162, 1975.

Forsyth, D.W., The evolution of the upper mantle beneath mid-ocean ridges, *Tectonophys.*, *38*, 89-118, 1977.

Knopoff, L., Observation and inversion of surface wave dispersion, *Tectonophysics*, *13*, 497-520, 1972.

Lamb, H., On the propagation of tremors over the surface of an elastic solid, *Phil. Trans. Roy. Soc. London*, *A203*, 1-42, 1904.

Patton, H., Crust and upper mantle structure of the Eurasian continent from the phase velocity and Q of surface waves, *Rev. Geophys. Space Phys.*, *18*, 605-625, 1980.

Takeuchi, H., and M. Saito, Seismic surface waves, in *Seismology: Surface waves and Earth oscillations (Methods in Computational Physics, vol. 11)*, ed. by B.A. Bolt, Academic Press, New York, 217-295, 1972.

Toks¨oz, N.M. and P. Bird, Formation and evolution of marginal basins and continental plateaus, in *Island arcs, Deep sea trenches and back-arc basins (Maurice Ewing Series vol.1)*, ed. by M. Talwani and W.C. Pitman III, American Geophysical Union, Washington, D.C., 379-393, 1977.